

Pseudodifferential Operators, Microlocal Analysis and Image Restoration*

Ryuichi Ashino[†] Steven J. Desjardins^{‡§}

Chris Heil[¶] Michihiro Nagase^{||}
Rémi Vaillancourt^{‡**}

CRM-2985

December 2003

*This research was partially supported by the Japanese Ministry of Education, Culture, Sports, Science and Technology, Grant-in-Aid for Scientific Research (B) 14340045(2002–2004), (C) 15540170(2003–2004), NSF Grant DMS-0139261, the Natural Sciences and Engineering Research Council of Canada and the Centre de recherches mathématiques of the Université de Montréal.

[†]Division of Mathematical Sciences, Osaka Kyoiku University, Kashiwara, Osaka 582-8582, Japan; ashino@cc.osaka-kyoiku.ac.jp

[‡]Department of Mathematics and Statistics, University of Ottawa, 585 King Edward Ave., Ottawa ON Canada K1N 6N5

[§]desjards@mathstat.uottawa.ca

[¶]School of Mathematics, Georgia Institute of Technology, Atlanta GA 30332 U.S.A.; heil@math.gatech.edu

^{||}Department of Mathematics, Graduate School of Science, Osaka University, Toyonaka, Osaka 560-0043, Japan; nagase@math.wani.osaka-u.ac.jp

^{**}remi@uottawa.ca

Abstract

Pseudodifferential operators with symbols supported on sectors of dyadic annuli in the Fourier domain are used to perform microlocal analysis of tempered distributions. Microlocal analysis is recalled. The above symbols are made of smooth wavelet frames which are constructed in the Fourier domain by means of modulated smooth tapered characteristic functions. The method is used to localize a line of singularities in an image.

1999 *Mathematics Subject Classification*. Primary 35S05; Secondary 35A27, 65T60

Keywords and Phrases. Pseudodifferential operator, microlocal analysis, smooth wavelet frame

To appear in *Advances in Pseudo-Differential Operators*, R. Ashino, P. Boggiotto and M. W. Wong, eds., Birkhäuser, Boston

Résumé

On fait l'analyse microlocale de distributions tempérées au moyen d'opérateurs pseudodifférentiels à symboles supportés dans des secteurs dyadiques dans le domaine de Fourier. Ces symboles sont faits d'ondelettes obliques lisses construites dans le domaine de Fourier au moyen de fonctions caractéristiques modulées et lissées. On utilise cette méthode pour localiser une ligne de singularités dans une image.

1 Introduction

Pseudodifferential operators whose symbols are modulated smooth tapered functions with support on sectors of dyadic annuli in the Fourier domain are designed to perform microanalysis of tempered distribution on \mathbb{R}^2 . These tapered functions form a smooth tight frame with frame bound 1, called *Parseval frame*.

Nonsmooth orthonormal multiwavelets have been constructed in [3] for performing microlocal analysis of tempered distributions in \mathbb{R}^n . The multiwavelets, whose Fourier transforms consist of characteristic functions of cubes, have perfect localization in the Fourier domain but poor localization in the x domain. To obtain good localization in both the x and Fourier domains in \mathbb{R}^n , in [4], the blockwavelets are smoothed by convolution and normalized to produce Parseval frames. In [5], [8], nonorthogonal rectangular and polar smooth frame wavelets in \mathbb{R}^2 are obtained from a multiresolution analysis. In [5], one also finds a general construction of microlocal frame wavelets supported on a general ring of sets surrounding the origin and whose dyadic dilations cover $\mathbb{R}^2 \setminus \{0\}$.

In [1], Aldroubi, Cabrelli, and Molter have constructed wavelets on irregular grids with arbitrary dilation matrices, and frame atoms for $L^2(\mathbb{R}^d)$.

In the present paper, attention is restricted to microlocal analysis in the two-dimensional case with the goal of localizing the singularities of a function f in the time domain by analyzing the growth of its Fourier transform, \widehat{f} , in wedges in the Fourier domain.

In view of numerical applications on domains with pixels at integer points, the continuous Fourier transform $\widehat{f}(\xi)$ of a function $f(x)$ defined over \mathbb{R}^2 and the inverse Fourier transform of $\widehat{f}(\xi)$ will be

$$\widehat{f}(\xi) = \int e^{-2\pi i \xi \cdot x} f(x) dx, \quad f(x) = \int e^{2\pi i x \cdot \xi} \widehat{f}(\xi) d\xi \quad (1)$$

and Plancherel's theorem will be

$$\langle f, g \rangle = \langle \widehat{f}, \widehat{g} \rangle, \quad (2)$$

where

$$\langle f, g \rangle = \int_{\mathbb{R}^2} f(x) \overline{g(x)} dx, \quad \langle \widehat{f}, \widehat{g} \rangle = \int_{\mathbb{R}^2} \widehat{f}(\xi) \overline{\widehat{g}(\xi)} d\xi.$$

Since wedges in \mathbb{R}^2 are generalizations of the positive real axis in \mathbb{R} , smooth frame wavelets are generalized to $L^2(\mathbb{R}^2)$ by properly tapering the Fourier transforms of the orthonormal multiwavelets given in [3]. Thus, the dyadically scaled Fourier transforms of the frame wavelets $\{\psi^\ell(x)\}$, $\ell = 1, 2, \dots, L$, satisfy the identity

$$G(\xi) := \sum_{\ell=1,2,\dots,12,j \in \mathbb{Z}} |\widehat{\psi}^\ell(2^j \xi)|^2 \equiv 1, \quad \xi \neq 0. \quad (3)$$

Our smooth frame wavelets can be derived from a frame multiresolution analysis by two-scale equations. However, they are not orthogonal to each other, nor to the spaces V_j spanned by the scaled and shifted scaling functions.

The paper proceeds as follows. In Section 2, the concepts of microlocal analysis are briefly reviewed. In Section 3, necessary and sufficient conditions are given to characterize tight frame wavelets. In Section 4, two-dimensional tapered characteristic functions are constructed. Section 5 introduces radial paving of the Fourier domain for microlocal analysis. In Section 6 an image restoration algorithm is described and the location of a line of singularities in an image is found by means of the frame coefficients.

2 Microlocal analysis

Our smooth tight frame wavelets are designed for investigating the microanalytic content of distributions. Hyperfunctions, which were introduced by Sato [13] and extensively developed by the Kyoto school of mathematics, can be considered intuitively as sums of boundary values of holomorphic functions defined in infinitesimal wedges (see [12] and the references therein).

We write $\mathbb{C}^2 = \mathbb{R}_x^2 + i\mathbb{R}_y^2$ and let Γ be a cone with vertex at the origin in \mathbb{R}_y^2 . If Δ is an open set in \mathbb{R}_y^2 which approaches Γ asymptotically near the origin from the interior of Γ , then the subset $U = \mathbb{R}^2 + i\Delta$ of \mathbb{C}^2 is called an *infinitesimal wedge* with opening Γ , and is denoted by $\mathbb{R}^2 + i\Gamma_0$ (see Fig. 1).

Let $f(x)$ be a “generalized boundary value” of a holomorphic function in an infinitesimal wedge $\mathbb{R}^2 + i\Gamma_0$; that is,

$$f(x) = \lim_{y \rightarrow 0, y \in \Gamma} f(x + iy) := f(x + i\Gamma_0).$$

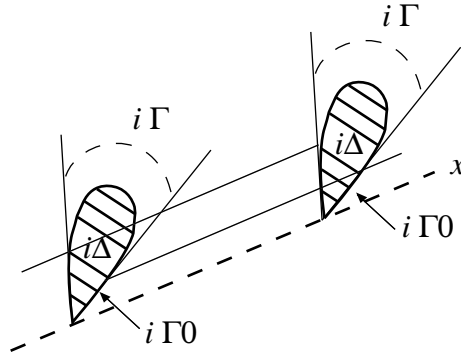


Figure 1: An infinitesimal wedge $\mathbb{R}^2 + i\Gamma_0$.

Definition 1. A distribution $f(x)$ is said to be analytic with respect to a direction ξ_0 if it can be represented as a finite sum of limits $f_j(x + i\Gamma_j 0)$ of slowly increasing holomorphic functions $f_j(z)$ in $\mathbb{R}^2 + i\Gamma_j 0$ such that, for every j , we have

$$\Gamma_j \cap \{y \in \mathbb{R}^2 ; y \cdot \xi_0 < 0\} \neq \emptyset.$$

To characterize the microanalyticity of a slowly increasing distribution $f \in \mathcal{S}'(\mathbb{R}^2)$ by its Fourier transform, \widehat{f} , we introduce the dual cone, Γ° , of the cone Γ defined by

$$\Gamma^\circ := \{\xi \in \mathbb{R}^2 ; y \cdot \xi \geq 0 \text{ for every } y \in \Gamma\}$$

(see Fig. 2); Γ° is a proper closed convex cone in \mathbb{R}^2 . The complement of Γ° is denoted by $(\Gamma^\circ)^c$.

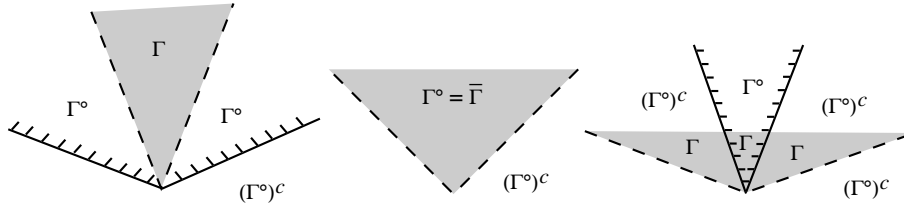


Figure 2: Open cone Γ , dual cone Γ° , and complement $(\Gamma^\circ)^c$ of dual cone.

The following lemma is standard (see [12]).

Lemma 1. Let Γ be an open convex cone. A slowly increasing distribution $f(x) \in \mathcal{S}'(\mathbb{R}^2)$ can be represented as the limit $f(x + i\Gamma 0)$ of a slowly increasing holomorphic function $f(z)$ in the convex hull of the infinitesimal wedge $\mathbb{R}^2 + i\Gamma 0$ if and only if the Fourier transform, \widehat{f} , of f is exponentially decreasing in the open cone $(\Gamma^\circ)^c$, the complement of Γ° ; that is, \widehat{f} is exponentially decreasing on every closed proper subcone $\Gamma' \subset \subset (\Gamma^\circ)^c$.

The larger the opening of Γ , the more regular a slowly increasing distribution $f(x + i\Gamma 0)$ will be. The cone Γ with largest opening is the whole space, in which case $f(x + i\Gamma 0)$ is analytic. For the next largest possible openings, Γ are half-spaces.

It is desirable to localize the directional decay of $\widehat{f}(\xi)$, because local nonsmoothness of a function $f(x)$ corresponds to slow decay of $\widehat{f}(\xi)$ along some directions at infinity. Each such direction corresponds to a point on the unit sphere \mathbb{S}^1 in ξ -space. Therefore, we shall use the coordinates $(x, \xi) \in \mathbb{R}^2 \times \mathbb{S}^1$ to represent a point $x \in \mathbb{R}^2$ together with a direction $\xi \in \mathbb{S}^1$.

Definition 2. A distribution $f(x) \in \mathcal{D}'(\mathbb{R}^2)$ is said to be analytic at $x_0 \in \mathbb{R}^2$ if there exists an open neighborhood $V \subset \mathbb{R}^2$ of x_0 such that the restriction $f|_V$ of f on V is analytic in V . The set of all points $x \in \mathbb{R}^2$ where f is not analytic is called the singular support of f .

Definition 3. A distribution $f(x)$ is said to be microanalytic or microlocal analytic at $(x_0, \xi_0) \in \mathbb{R}^2 \times \mathbb{S}^1$ if there exists a distribution $g(x)$ which is analytic with respect to the direction ξ_0 such that $f(x) - g(x)$ is analytic in a neighborhood of x_0 . The set of all points $(x, \xi) \in \mathbb{R}^2 \times \mathbb{S}^1$ where f is not microanalytic is called the singular spectrum of f .

3 Necessary and sufficient conditions for tight frame wavelets

We refer to [7], [10] for detailed background on frames.

Definition 4. Let I be an index set. A sequence of vectors $\{f_i\}_{i \in I}$ in a Hilbert space H is called a frame for H if there exist constants $A, B > 0$ (called frame bounds) such that

$$\forall f \in H, \quad A \|f\|^2 \leq \sum_{i \in I} |\langle f, f_i \rangle|^2 \leq B \|f\|^2.$$

If $A = B$, the frame is said to be an A -tight frame. A 1-tight frame is called a Parseval frame.

It can be shown that $\|f_i\|^2 \leq B$ for each $i \in I$. Further, $\{f_i\}_{i \in I}$ is a tight frame with frame bound A if and only if

$$\forall f \in H, \quad \sum_{i \in I} \langle f, f_i \rangle f_i = Af.$$

A frame is *redundant* if it is possible to remove some element from the frame and still leave a complete set. For the case of tight frames, we can give the following easy characterization of redundancy. Redundancy of frames is explored in more detail in [6].

Lemma 2. Let $\{f_i\}_{i \in I}$ be an A -tight frame for a Hilbert space H . If $j \in I$ is such that $\|f_j\|^2 < A$, then $\{f_i\}_{i \neq j}$ is still a frame for H , with frame bounds $A' = A - \|f_j\|^2$ and $B' = A$.

Proof. If $f \in H$, then clearly

$$\sum_{i \neq j} |\langle f, f_i \rangle|^2 \leq \sum_{i \in I} |\langle f, f_i \rangle|^2 = A \|f\|^2.$$

This establishes the upper frame bound. On the other hand, using the Cauchy-Schwarz inequality, we have

$$\begin{aligned} \sum_{i \neq j} |\langle f, f_i \rangle|^2 &= \sum_{i \in I} |\langle f, f_i \rangle|^2 - |\langle f, f_j \rangle|^2 \\ &\geq A \|f\|^2 - \|f\|^2 \|f_j\|^2 = (A - \|f_j\|^2) \|f\|^2, \end{aligned}$$

which establishes the lower frame bound. □

Given $f \in L^2(\mathbb{R}^2)$, let $f_{j,k}(x)$ denote the scaled and shifted function

$$f_{j,k}(x) = 2^j f(2^j x - k), \quad j \in \mathbb{Z}, \quad k \in \mathbb{Z}^2,$$

with Fourier transform

$$\widehat{f}_{j,k}(\xi) = e^{-2\pi i k \cdot \xi} 2^{-j} \widehat{f}(2^{-j} \xi).$$

Let \mathbb{L} be a finite index set. A system $\{\psi_{j,k}^\ell\}_{\ell \in \mathbb{L}, j \in \mathbb{Z}, k \in \mathbb{Z}^2} \subset L^2(\mathbb{R}^2)$ is called an A -tight wavelet frame if

$$f(x) = \frac{1}{A} \sum_{\ell \in \mathbb{L}, j \in \mathbb{Z}, k \in \mathbb{Z}^2} \langle f, \psi_{j,k}^\ell \rangle \psi_{j,k}^\ell(x), \quad \forall f \in L^2(\mathbb{R}^2). \quad (4)$$

A system $\{\psi_{j,k}^\ell\}_{\ell \in \mathbb{L}, j \in \mathbb{Z}, k \in \mathbb{Z}^2} \subset L^2(\mathbb{R}^2)$ is called an *orthonormal wavelet basis* if it is an orthonormal basis for $L^2(\mathbb{R}^2)$. An extension of Lemma 2 shows that this is equivalent to saying that the system $\{\psi_{j,k}^\ell\}_{\ell \in \mathbb{L}, j \in \mathbb{Z}, k \in \mathbb{Z}^2}$ is a Parseval wavelet frame and $\|\psi^\ell\|_{L^2(\mathbb{R}^2)} = 1$ for $\ell \in \mathbb{L}$.

The following general theorem, which is stated and proved for \mathbb{R}^n in [9, Theorem 1], gives necessary and sufficient conditions to have a Parseval wavelet frame in \mathbb{R}^2 .

Theorem 1. If $\{\psi^1, \psi^2, \dots, \psi^L\} \subset L^2(\mathbb{R}^2)$, then

$$\|f\|_{L^2(\mathbb{R}^2)}^2 = \sum_{\ell \in \mathbb{L}, j \in \mathbb{Z}, k \in \mathbb{Z}^2} |\langle f, \psi_{j,k}^\ell \rangle|^2 \quad (5)$$

for all $f \in L^2(\mathbb{R}^2)$ if and only if the functions $\{\psi^1, \psi^2, \dots, \psi^L\}$ satisfy the following two equalities:

$$\sum_{\ell \in \mathbb{L}, j \in \mathbb{Z}} \left| \widehat{\psi}^\ell(2^j \xi) \right|^2 = 1, \quad \text{a.e. } \xi \in \mathbb{R}^2, \quad (6)$$

$$\sum_{\ell \in \mathbb{L}, j \in \mathbb{Z}_+} \widehat{\psi}^\ell(2^j \xi) \overline{\widehat{\psi}^\ell(2^j(\xi + q))} = 0, \quad \text{a.e. } \xi \in \mathbb{R}^2, \quad \forall q \in \mathbb{Z}^2 \setminus (2\mathbb{Z})^2, \quad (7)$$

where $\mathbb{Z}_+ := \mathbb{N} \cup \{0\}$ and $q \in \mathbb{Z}^2 \setminus (2\mathbb{Z})^2$ means that at least one component q_j is odd.

Corollary 1. *Under the hypotheses of Theorem 1, any function $f \in L^2(\mathbb{R}^2)$ admits the tight wavelet frame expansion*

$$f(x) = \sum_{\ell \in \mathbb{L}, j \in \mathbb{Z}, k \in \mathbb{Z}^2} \langle f, \psi_{j,k}^\ell \rangle \psi_{j,k}^\ell(x). \quad (8)$$

By using the localization property of the frame wavelet in the Fourier domain, one can study the directions of growth of $\widehat{f}(\xi)$ by looking at the size of the frame coefficients

$$\langle f, \psi_{j,k}^\ell \rangle = \langle \widehat{f}, \widehat{\psi}_{j,k}^\ell \rangle. \quad (9)$$

Moreover, by using the localization property of the frame wavelets in x -space, one can localize the singular support of $f(x)$ by varying ℓ , j and k in (9).

An alternate formulation of the problem is by means of a pseudodifferential operator

$$\begin{aligned} Pf(x) &= \int \left(\sum_{j,k,\ell} \psi_{j,k}^\ell(x) \overline{\widehat{\psi}_{j,k}^\ell(\xi)} \right) \widehat{f}(\xi) d\xi \\ &= \int e^{2\pi i x \cdot \xi} \left(\sum \psi_{j,k}^\ell(x) e^{-2\pi i(k+x) \cdot \xi} 2^{-j} \overline{\widehat{\psi}^\ell(2^{-j}\xi)} \right) \widehat{f}(\xi) d\xi \\ &= \int e^{2\pi i x \cdot \xi} p(x, \xi) \widehat{f}(\xi) d\xi, \end{aligned} \quad (10)$$

The problem is to find a symbol p such that Pf is strongly localized on the singular support of f and negligible where f is smooth. Pseudodifferential operators with smooth symbols do not extend the singular support of f ; that is, the singular support of Pf is contained in the singular support of f . In Section 6, the symbol will involve only the matrix Q_j^ℓ which will be a discretized version of $\widehat{\psi}_j^\ell(\xi) = \widehat{\psi}^\ell(2^{-j}\xi)$, and the values of the shift parameter k in the summation in (8) will be determined indirectly by the singular support of f through the size of $|\langle \widehat{f}, \widehat{\psi}_{j,k}^\ell \rangle|$.

4 Two-dimensional tapered characteristic functions

The localization property of frame wavelets in the Fourier domain by means of the frame coefficients (9) depends upon the support of the wavelet functions $\widehat{\psi}_{j,k}^\ell$ on appropriate rectangular or polar pavings of the plane.

In this section, we construct rectangular paving as a stepping stone for polar paving in section 5.

We first define bell functions of one variable. We partition the s axis with points $\{a_j\}$ ($a_j < a_{j+1}$) into intervals, such that the j th interval is $[a_j, a_{j+1}]$ and has length $L_j = a_{j+1} - a_j$. Around each endpoint of an interval, say a_j , we allow a *transition region* $[a_j - \varepsilon_j, a_j + \varepsilon_j]$ of width $2\varepsilon_j$; in this region, the bell function $b_j(s)$ over the interval j rises smoothly from 0 to 1, and the bell function $b_{j-1}(s)$ over the interval $j-1$ decreases smoothly from 1 to 0. The bell function $b_j(s)$ is nonzero for s in the region $(a_j - \varepsilon_j, a_{j+1} + \varepsilon_{j+1})$ and it is 1 for s in $[a_j + \varepsilon_j, a_{j+1} - \varepsilon_{j+1}]$. Bell functions over two adjacent intervals overlap in their transition region.

A bell function, or window, $b_j(s)$ has the following properties:

(i) $0 \leq b_j(s) \leq 1$ for all s and

$$b_j(s) = \begin{cases} 1 & \text{if } a_j + \varepsilon_j \leq s \leq a_{j+1} - \varepsilon_{j+1} \\ 0 & \text{if } s \leq a_j - \varepsilon_j \text{ or } s \geq a_{j+1} + \varepsilon_{j+1} \end{cases}$$

where $\varepsilon_j \geq 0$ and $\varepsilon_j + \varepsilon_{j+1} \leq L_j$;

(ii) $b_j^2(a_j + s) + b_j^2(a_j - s) = 1$ if $|s| \leq \varepsilon_j$;

(iii) $b_j(a_j + s) = b_{j-1}(a_j - s)$ if $|s| \leq \varepsilon_j$.

Condition (i) says that the windows are simply smoothed versions of the rectangular window and b_j can be specified if it is known in the left transition region $LTR = [a_j - \varepsilon_j, a_j + \varepsilon_j]$ and the right transition region $RTR = [a_{j+1} - \varepsilon_{j+1}, a_{j+1} + \varepsilon_{j+1}]$. So we need only consider the window function in the transition regions; we refer to this as a *taper function*. We shall denote the restrictions of b_j on LTR and RTR by

$$t_l(s; \varepsilon_j) = b_j(s) \quad \text{for } s \in [a_j - \varepsilon_j, a_j + \varepsilon_j] \quad (11)$$

and

$$t_r(s; \varepsilon_j) = b_j(s) \quad \text{for } s \in [a_{j+1} - \varepsilon_{j+1}, a_{j+1} + \varepsilon_{j+1}], \quad (12)$$

respectively.

The left part of Fig. 3 shows three tapered characteristic functions: (a) of the interval $[0, 1]$ with transition width $1/2$ at both ends, (b) of the interval $[1, 2]$ with transition widths $1/2$ at the left end and 1 at the right end, and (c) of the interval $[2, 4]$ with transition widths 1 at the left end and 2 at the right end. It is seen in the right part of Fig. 3 that the square root of the sum of the squares of these three functions is equal to 1 over the overlapping tapered parts.

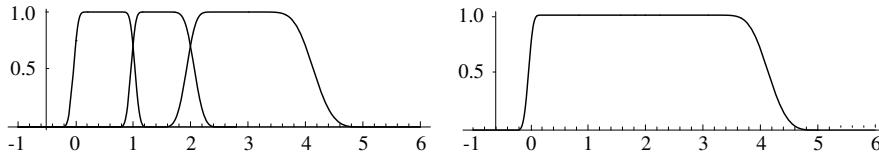


Figure 3: Left: three overlapping tapered characteristic functions. Right: square root of sum of squares of the three functions.

Bell functions of two variables are defined as the tensor product of two bell functions of one variable,

$$b(s_1, s_2) = b_1(s_1)b_2(s_2),$$

where b_1 and b_2 have transition regions of appropriate lengths at their left and right ends.

We illustrate two-dimensional paving of the Fourier domain by the following example. The tapered characteristic functions of the 12 squares of side $1/2$ of the ring $\mathcal{R}^{[0]}$, shown in Fig. 4, have transition widths 4ε on the outside edges and 2ε on all the other edges. Similarly, the three squares of side 1 of the second ring $\mathcal{R}^{[1]}$ in the first quadrant,

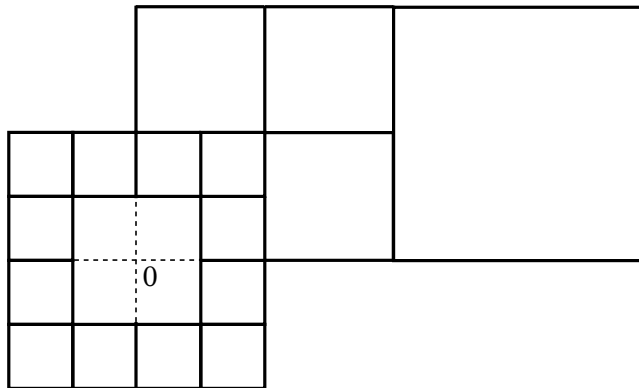


Figure 4: Paving of the Fourier domain by rings of 12 dyadic squares.

produced by dilation by 2, have transition widths 8ε on the four outside edges and 4ε on the remaining edges.

In general, the ring $\mathcal{R}^{[j]}$, parametrized by $j \in \mathbb{Z}$, is the support of tapered characteristic functions

$$\widehat{\psi}_j^\ell(\xi) := \widehat{\psi}^\ell(2^j \xi), \quad \ell = 1, 2, \dots, 12,$$

where the Fourier transform is defined by (1). For fixed j , the only rings that intersect with $\mathcal{R}^{[j]}$ are $\mathcal{R}^{[j-1]}$ and $\mathcal{R}^{[j+1]}$. Given one ring $\mathcal{R}^{[j]}$, the other rings are simply obtained by dilation.

To prove identity (3), one needs only check points where two, three and four tapered wavelet frame functions overlap. Let us check identity (3) at an arbitrary point ξ in the intersection of the four tapered parts of $\widehat{\psi}_1^2$ and $\widehat{\psi}_2^\ell$, $\ell = 1, 2, 3$. Since tapering is of the same width for all four transition regions, it is obtained by the same taper functions (11) and (12), $t_l(s, \varepsilon)$ and $t_r(s, \varepsilon)$, respectively. Proceeding counter-clockwise from the top right corner of the frame $\widehat{\psi}_1^2$, we have

$$\begin{aligned} & t_r(\xi, \varepsilon)^2 t_r(\xi, \varepsilon)^2 + t_r(\xi, \varepsilon)^2 t_l(\xi, \varepsilon)^2 + t_l(\xi, \varepsilon)^2 t_l(\xi, \varepsilon)^2 + t_l(\xi, \varepsilon)^2 t_r(\xi, \varepsilon)^2 \\ &= t_r(\xi, \varepsilon)^2 [t_r(\xi, \varepsilon)^2 + t_l(\xi, \varepsilon)^2] + t_l(\xi, \varepsilon)^2 [t_l(\xi, \varepsilon)^2 + t_r(\xi, \varepsilon)^2] \\ &= t_r(\xi, \varepsilon)^2 + t_l(\xi, \varepsilon)^2 \\ &= 1. \end{aligned}$$

We generalize to two dimensions the treatment of smooth frames for $H^2(\mathbb{R})$ given in [11, Section 8.4] and show that the functions $\psi_{j,k}^\ell$ form a Parseval wavelet frame for $L^2(\mathbb{R}^2)$.

Theorem 2. *If $0 < \varepsilon \leq 1/4$, the system $\{\psi_{j,k}^\ell\}$, $j \in \mathbb{Z}$ and $k \in \mathbb{Z}^2$, is a Parseval wavelet frame for $L^2(\mathbb{R}^2)$.*

Proof. Identity (3) has just been proved. For $f \in L^2(\mathbb{R}^2)$, a similar argument to the proof of Theorem 2 implies

$$\sum_{k \in \mathbb{Z}^2} |\langle f, \psi_{j,k}^\ell \rangle|^2 = \int |\widehat{f}(\xi)|^2 |\widehat{\psi}^\ell(2^{-j}\xi)|^2 d\xi$$

and

$$\begin{aligned} \sum_{\ell=1}^{12} \sum_{j=-\infty}^{\infty} \sum_{k \in \mathbb{Z}^2} |\langle f, \psi_{j,k}^\ell \rangle|^2 &= \sum_{\ell=1}^{12} \sum_{j=-\infty}^{\infty} \int |\widehat{f}(\xi)|^2 |\widehat{\psi}^\ell(2^{-j}\xi)|^2 d\xi \\ &= \int |\widehat{f}(\xi)|^2 d\xi = \|f\|_{L^2(\mathbb{R}^2)}^2. \end{aligned}$$

A folding argument [11, p. 419], shows that

$$\|\psi_{0,0}^\ell\|_{L^2(\mathbb{R}^2)}^2 = \frac{1}{4}.$$

Thus we have a family of frames in $L^2(\mathbb{R}^2)$ that do not form an orthonormal basis. □

5 Radial paving of the Fourier domain for microlocal analysis

To have arbitrarily fine angular resolutions in the Fourier domain it is convenient to consider polar pavings of the plane by dyadic sectors of annuli with appropriate angular divisions. A few sectors of annuli of the first and second dyadic rings are shown in Fig. 5.

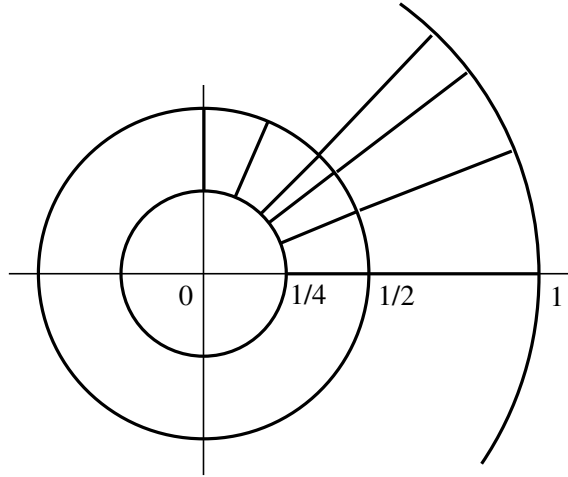


Figure 5: Dyadic sectors of annuli with central disk in the Fourier domain. Unequal angular divisions offer directional freedom.

It is to be noticed that the radial interval is of the form $[r, 2r]$. Polar wavelets can be defined by the inverse Fourier transforms of nonoverlapping characteristic functions over sectors of annuli. If the Fourier domain is completely covered by L nonoverlapping wedges, the L family of wavelets $\{\psi_{j,k}^\ell\}$, with $\ell = 1, \dots, L$, $j \in \mathbb{Z}$, and $k \in \mathbb{Z}^2$, form an orthonormal basis of $L^2(\mathbb{R}^2)$. This basis can be generated by a frame multiresolution analysis with scaling functions.

To have better localization in x -space, these functions are tapered with width 2ε on the inside arcs, width 4ε on the outside arcs and width εs , $r \leq s \leq 2r$, on the straight radial edges. Provided ε is sufficiently small so that tapering overlaps are restricted to immediately adjacent regions, it will be shown below that identity (3) is satisfied. By taking a ring sufficiently close to the origin, by construction, dyadic polar rings form a Parseval frame.

The description of polar frame wavelets is considerably simplified by using the polar coordinates (r, θ) in the Fourier domain instead of the Cartesian coordinates (ξ_1, ξ_2) . The inverse and direct coordinate transformations are

$$\xi_1 = r \cos 2\pi\theta, \quad \xi_2 = r \sin 2\pi\theta; \quad r = \sqrt{\xi_1^2 + \xi_2^2}, \quad \theta = \frac{1}{2\pi} \arctan\left(\frac{\xi_2}{\xi_1}\right),$$

with the appropriate branches of arctan. In the (r, θ) -plane, the polar frame wavelets are supported in the semi-infinite strip $\{0 \leq r < \infty, 0 \leq \theta \leq 1\}$, and are 1-periodic in θ . The strip, shown in Fig. 6, is divided into rectangles with vertical sides at $r = 2^j$, $j \in \mathbb{Z}$ and horizontal sides at

$$0 = \theta_0 < \theta_1 < \dots < \theta_\ell < \dots < \theta_L = 1.$$

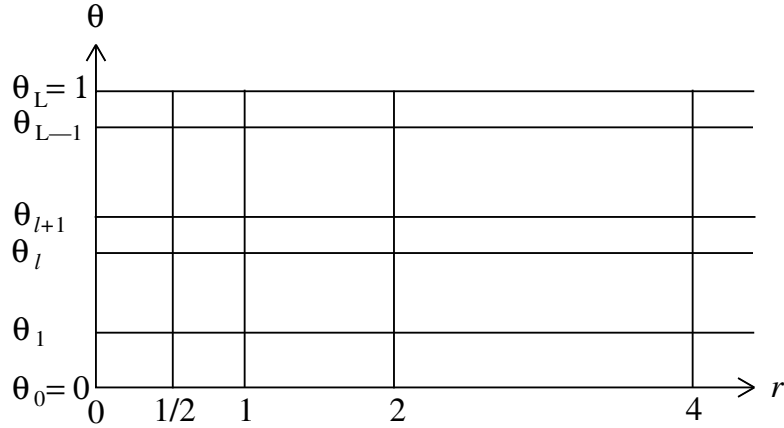


Figure 6: Strip in the (r, θ) -plane.

The smooth functions $\widehat{\psi}_j^\ell(r, \theta) = \widehat{\psi}^\ell(2^{-j}r, \theta)$ are easily obtained by tapering the characteristic functions of each rectangle. Tapering is done along vertical sides with transition regions of width $2^{j+1}\varepsilon$ at $r = 2^{j-1}$ and along horizontal sides with transition regions of width $2\varepsilon_\ell$ with $\varepsilon_L = \varepsilon_0$ at $\theta = \theta_L$.

It is then clear that identity (3) is satisfied.

It is shown in [5] that our smooth frame wavelets can be obtained from a frame multiresolution analysis with scaling functions.

6 A numerical implementation of the localization method

In this section, we describe how to apply the above theory to the restoration of finite images represented by matrices. Since the Fourier transform of a finite region gives rise to oscillations of the cardinal sine type, care must be taken in the restoration process.

The restoration process described in [5] involves the following steps.

- (a) A scarred image (A) is to be restored as its original image (F).
- (b) Image (A) is Fourier transformed and filtered by multiplication with tapered characteristic functions with support far from the origin and at right angles to the singularities to be localized. This produces image (B).
- (c) The frame coefficients (9) in the Fourier domain,

$$\langle \widehat{f}, \widehat{\psi}_{j,k}^\ell \rangle = \langle f, \psi_{j,k}^\ell \rangle,$$

make image (C).

- (d) In view of the Plancherel theorem, image (C) is used in the x domain to obtain the wavelet frame expansion (8) of Corollary 1. This produces a thick image (D) of the singularities in image (A)
- (e) The extra width of (D), caused by the side lobes in the support of $\psi_{j,k}^\ell$, is narrowed to eliminate oscillations due to the cardinal sine effect when transforming functions with finite support. This is image (E).
- (f) A tuned multiple of (E) is subtracted from (A) to restore the original image (F).

In the case of polar frames, two-dimensional bell functions were produced by the Mathematica Wavelet Explorer by tapering characteristic functions over the rectangles with left and right vertical edges at $r = 1/2$ and $r = 1$ with horizontal transition widths $1/8$ and $1/4$, respectively. The lower and upper transition widths of the rectangle with lower and upper horizontal edges at θ_ℓ and $\theta_{\ell+1}$ are $(\theta_\ell - \theta_{\ell-1})/4$ and $(\theta_{\ell+1} - \theta_\ell)/4$, respectively.

Tapering was done by iterating the sine function twice to get

$$b(s) = \sin\left(\frac{\pi}{2} \sin^2\left(\frac{\pi}{2} \sin^2\left(\frac{\pi}{2} s\right)\right)\right)$$

with the option `Taper -> {Trig[2], epsilon}`. It is easy to see that

$$b(s)^2 + b(1-s)^2 = 1, \quad s \in [0, 1],$$

by noting that $\sin((\pi/2)(1-s)) = \cos((\pi/2)s)$ and repeated use of the identity $\cos^2 s = 1 - \sin^2 s$.

Six sets of longer rectangles were produced by horizontal dyadic scaling of the functions of the first set. The support of these functions is a strip with far right end at $r = 287$.

These functions are evaluated in the form of tables by Mathematica in the (ξ_1, ξ_2) plane and exported to MATLAB in the form of matrices:

$$Q_1^1, \dots, Q_1^L, \dots, Q_7^1, \dots, Q_7^L.$$

By construction, the top right 87×87 matrix Q_7^d (d for diagonal), with center line making an angle of $\pi/4$ radians with respect to the ξ_1 axis, has lower left and upper right elements in positions $(87, 201)$ and $(1, 287)$. Therefore, in the sequel we shall work with matrices of dimension 287×287 .

A diagonal line is added to the Saturn image making (A) shown in the top left part of Fig. 7.

Let f be the matrix representing image (A). The discrete Fourier transform F of f is filtered by means of the top right frame, Q_7^d , of the fifth ring to recover the singularity and eliminate the smooth part of the image. We write $k = (k_1, k_2)$. Let the (m, n) -th element of the matrix of exponentials E_k be

$$E_k(m, n) = e^{-2\pi i(m-1, n-1) \cdot (k_1, k_2)/287}. \quad (13)$$

Discretizing the scalar product (9),

$$\langle \hat{f}, \hat{\psi}_{5,k}^d \rangle,$$

we obtain the matrix $C = (c_k)$ of frame coefficients

$$c_k = \sum_{m,n=1}^{287} (F.*E_k.*Q_7^d)(m, n), \quad k_1 = k_2 = 1, \dots, 287, \quad (14)$$

where $*$ denotes componentwise matrix multiplication. Note that Q_7^d is a real matrix. The matrix C represents image (C).

Discretizing the partial sum (8),

$$\sum_{k_1=k_2=1}^{287} \langle \hat{f}, \hat{\psi}_{5,k}^d \rangle \hat{\psi}_{5,k}^d(\xi),$$

we obtain the matrix $W = (w_k)$ of the wavelet frame expansion of the discrete inverse Fourier transform of the filtered image (B). The entries of W are

$$w_k = \left(\sum_{k_1=k_2=1}^{287} c_{m_1, m_1} E_{-m_1, -m_1}.*Q_7^d \right)_k, \quad (15)$$

where summation is over the diagonal segment S .

Since the Fourier transform of the smooth component of the image is localized mainly near the origin and the Fourier transform of the singularity consists mainly of details with high frequency, the properly modulated matrix filter Q_7^d picks up only the singularity.

The frame $\hat{\psi}_{5,k}^d(\xi)$, with support in the top right corner in the Fourier domain, picks up the singularities across segments parallel to the main diagonal.

In the top left part of Fig. 7, a diagonal line of height 100 has been added to the Saturn image making image (A). The Fourier transform of this image is filtered by a smooth polar frame supported on a sector of an annulus of aperture of 0.02π radians and inner and outer radii 220 and 287, along the secondary diagonal in the upper right corner of a 287×287 matrix in the Fourier domain and shown in the top right part of the figure (image (B)). The image of the frame coefficients of the filtered image is shown in the bottom left part of the figure (image (C)). This image clearly locates the diagonal line singularity added to the Saturn image. The bottom right part of the figure shows the frame expansion of the filtered image in the x domain (image (D)). It is seen that the smooth image has been filtered out.

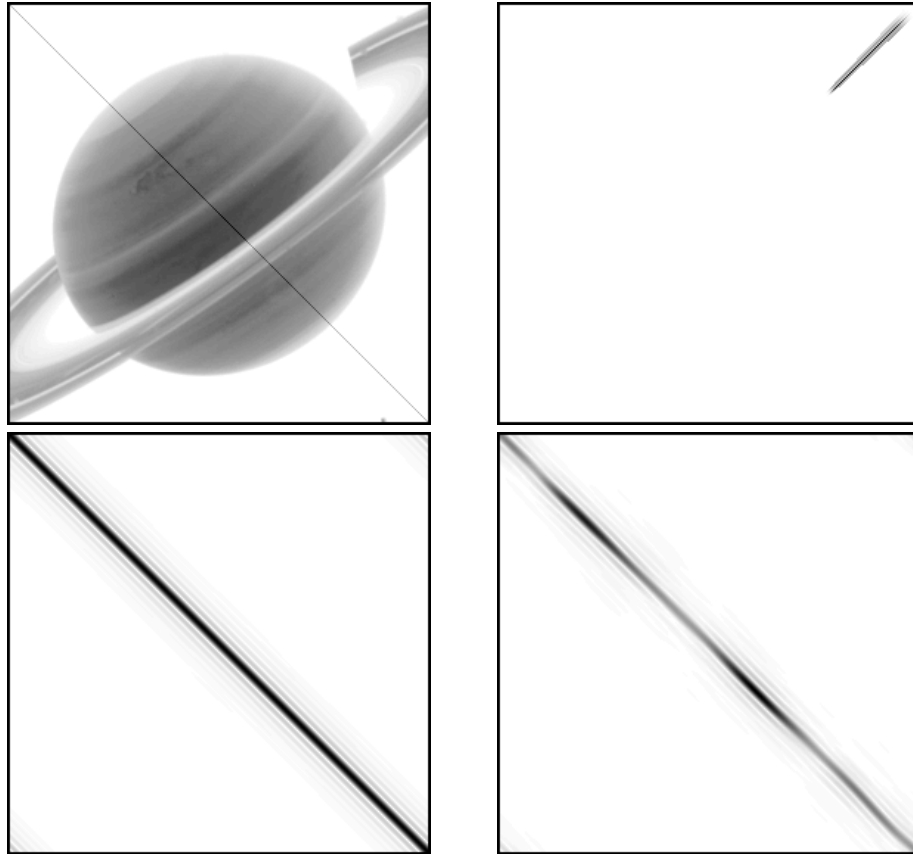


Figure 7: Top left: framed negative image of diagonal line added to the Saturn image. Top right: framed negative image of the filtered image in the Fourier domain. Bottom left: framed negative image of the frame coefficients of the filtered image in the Fourier domain. Bottom right: framed negative image of the frame reconstruction of the filtered image in the x domain.

References

- [1] A. Aldroubi, C. Cabrelli, U. M. Molter, *Wavelets on irregular grids with arbitrary dilation matrices, and frame atoms for $L^2(\mathbb{R}^d)$* , manuscript, (2003).
- [2] R. Ashino, C. Heil, M. Nagase, and R. Vaillancourt, *Microlocal analysis and multiwavelets in Geometry, Analysis and Applications*, (Varanasi 2000), R. S. Pathak, ed., World Sci. Publishing, River Edge, NJ, 2001, 293–302.
- [3] R. Ashino, C. Heil, M. Nagase, and R. Vaillancourt, *Microlocal filtering with multiwavelets*, *Comput. Math. Appl.* **41** (2001) 111–133.
- [4] R. Ashino, S. J. Desjardins, C. Heil, M. Nagase, and R. Vaillancourt, *Microlocal analysis, smooth frames and denoising in Fourier space*, *J. of Asian Information-Science-Life* **1**(2) (2002) 153–160.
- [5] R. Ashino, S. J. Desjardins, C. Heil, M. Nagase, and R. Vaillancourt, *Smooth tight frame wavelets and image microanalysis in the Fourier domain*, *Comput. Math. Appl.* **45** (2003) 1551–1579.
- [6] R. Balan, P. G. Casazza, C. Heil, and Z. Landau, *Deficits and excesses of frames*, *Adv. Comput. Math.* **18**, (2003) 93–116.
- [7] I. Daubechies, *Ten Lectures on Wavelets*, Society for Industrial and Applied Mathematics, Philadelphia PA, 1992.
- [8] S. J. Desjardins, *Image Analysis in Fourier Space*, Ph.D. Thesis, University of Ottawa, Ottawa, ON Canada, 2002.
- [9] M. Frazier, G. Garrigós, K. Wang, and G. Weiss, *A characterization of functions that generate wavelet and related expansion*, *J. Fourier Anal. Appl.* **3** (1997) 883–906
- [10] C. Heil and D. F. Walnut, *Continuous and discrete wavelet transforms*, *SIAM Rev.* **31** (1989) 628–666.
- [11] E. Hernández and G. Weiss, *A First Course on Wavelets*, CRC Press, Boca Raton FL, 1996.
- [12] A. Kaneko, *Microlocal analysis*, in *Encyclopaedia of Mathematics*, Kluwer Academic Publishers, Dordrecht, 1997.
- [13] M. Sato, *Theory of hyperfunctions I*, *J. Fac. Sci. Univ. Tokyo, Sec. I* **8** (1959) 139–193